Analytica Chimica Acta xxx (2015) 1–10

Contents lists available at ScienceDirect

Analytica Chimica Acta

journal homepage: www.elsevier.com/locate/aca

# Real-time prostate-specific antigen detection with prostate-specific antigen imprinted capacitive biosensors

Gizem Ertürk [a, b, 1], Martin Hedström [a, d], M. Aşkın Tümer [b], Adil Denizli [c], Bo Mattiasson [a, d, *]

[a] Department of Biotechnology, Lund University, Lund, Sweden
[b] Department of Biology, Hacettepe University, Ankara, Turkey
[c] Department of Chemistry, Hacettepe University, Ankara, Turkey
[d] CapSenze HB, Medicon Village, SE-223 63 Lund, Sweden

## HIGHLIGHTS

- Microcontact imprinting method was used for preparing the sensor chip for capacitive biosensing.
- High sensitivity was obtained.
- Good selectivity was demonstrated.
- Stability of the sensor chip was better than that of a corresponding antibody based assay.

## GRAPHICAL ABSTRACT

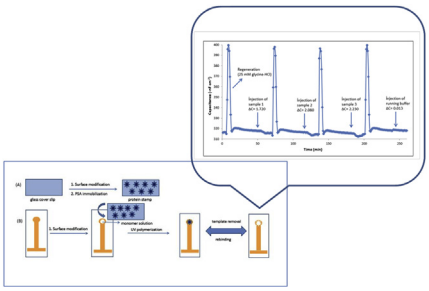

## ARTICLE INFO

*Article history:*
Received 14 November 2014
Received in revised form
19 July 2015
Accepted 24 July 2015
Available online xxx

*Keywords:*
Prostate cancer
Prostate-specific antigen detection
Microcontact imprinting
Immobilization
Ultraviolet-polymerization

## ABSTRACT

Prostate specific antigen (PSA) is a valuable biomarker for early detection of prostate cancer, the third most common cancer in men. Ultrasensitive detection of PSA is crucial to screen the prostate cancer in an early stage and to detect the recurrence of the disease after treatment. In this report, microcontact-PSA imprinted (PSA-MIP) capacitive biosensor chip was developed for real-time, highly sensitive and selective detection of PSA. PSA-MIP electrodes were prepared in the presence of methacrylic acid (MAA) as the functional monomer and ethylene glycol dimethacrylate (EGDMA) as the cross-linker via UV polymerization. Immobilized Anti-PSA antibodies on electrodes (Anti-PSA) for capacitance measurements were also prepared to compare the detection performances of both methods. The electrodes were characterized by atomic force microscopy (AFM), scanning electron microscopy (SEM) and cyclic voltammetry (CV) and real-time PSA detection was performed with standard PSA solutions in the concentration range of 10 fg $mL^{-1}$ −100 ng $mL^{-1}$. The detection limits were found as $8.0 \times 10^{-5}$ ng $mL^{-1}$ ($16 \times 10^{-17}$ M) and $6.0 \times 10^{-4}$ ng $mL^{-1}$ ($12 \times 10^{-16}$ M) for PSA-MIP and Anti-PSA electrodes, respectively. Selectivity studies were performed against HSA and IgG and selectivity coefficients were calculated. PSA detection was also carried out from diluted human serum samples and finally, reproducibility of the electrodes was tested. The results are promising and show that when the sensitivity of the capacitive system is combined with the selectivity and

* Corresponding author. Department of Biotechnology, Lund University, Lund, Sweden.
*E-mail address:* Bo.Mattiasson@biotek.lu.se (B. Mattiasson).
[1] On leave from Department of Biology, Hacettepe University, Ankara, Turkey.

http://dx.doi.org/10.1016/j.aca.2015.07.055
0003-2670/

reproducibility of the microcontact-imprinting procedure, the resulting system might be used successfully for real-time detection of various analytes even in very low concentrations.



## 1. Introduction

Prostate cancer accounts for approximately 10% of all deaths from cancer and it is the third most common cancer in men [1–3]. There are not any effective cures for the treatment of prostate cancer in the advanced metastatic stage [4]. Due to this, to reduce the mortality rate, early detection of this cancer is crucial [5]. Prostate specific antigen (PSA) is a valuable biomarker for the detection of prostate cancer [6]. PSA is a serine protease and normally found in serum. It is produced by the prostate epithelium and is responsible for the liquefaction of seminal fluid [7]. A total PSA level of 4.0 ng $mL^{-1}$ (more recently 2.5 ng $mL^{-1}$) is a highly probable indication for prostate cancer and it might indicate the need for biopsy [8–10]. PSA is not a cancer-specific marker since PSA level in serum might increase also in other non-cancerous diseases of prostate [1–3]. However, there is not an alternative marker instead of PSA for early detection of prostate cancer. Measurement of PSA level is not only used for the early detection of the cancer but also to monitor the response of the patients to the therapy [11]. In this case, detectable level of PSA indicates the recurrence of the disease. When using ultrasensitive assays, it is possible to either use very small sample volumes, or to dilute the sample such that background activities are markedly reduced. For this reason, ultrasensitive detection of serum PSA level especially in low pg $mL^{-1}$ region facilitates an early detection of prostate cancer and also recurrence of the disease [12–14].

Most of the current PSA assays are variants of enzyme linked immunosorbent assay (ELISA) in which it is necessary to use enzymatic, fluorescent or chemiluminescent labels to detect in a tedious and expensive way. Developing a biosensor for PSA detection offers an attractive possibility to create a point-of-care testing device to screen for prostate cancer in real-time [12,15,16]. Thus, the need for sample transport and delays associated with the central laboratories would be eliminated.

Affinity biosensors are based on binding interaction between the biorecognition element on the sensor chip and the analyte of interest. It is possible to assay biomacromolecules at very low concentrations with highly sensitive affinity biosensors [17]. Among label-free affinity biosensors, capacitive biosensors are used for quantifying biomolecular interactions real-time, label-free and in a fast, sensitive and selective manner [18–20]. Capacitive biosensors are the type of electrochemical sensors and the measurement is based on the change in the dielectric properties of the sensor surface when an analyte interacts with the biorecognition element, causing a decrease in capacitance [21,22]. Capacitive biosensors have been used for detection of a variety of different analytes [23–27].

Molecular imprinting is the technique growing in popularity for the design of biomimetic sensor layers during the last decade [28]. This is the technique of forming artificial recognition sites complementary to a “template” molecule by the polymerization of a monomer around the template [29–31]. The advantages of the technique including coping with complex matrices under tough conditions, reusability, cost-effective fabrication, high recognition capacity to the template molecule and binding characteristics almost as good as those of natural antibodies make it promising to use in a variety of areas, such as solid-phase extraction, chiral separation, catalysis, library screening, drug-delivery, biosensors [32–36].

In the study reported here, a capacitive biosensor with an automated-flow injection system was developed for PSA detection. A microcontact imprinting method was used for imprinting of PSA onto the capacitive sensor surface. To our knowledge, this is the first microcontact-PSA imprinting study for the detection of PSA. Microcontact imprinting is a surface coating technique used for the creation of recognition cavities for the macromolecular templates [37–40]. In the general procedure, target protein is immobilized onto a glass support to form the protein stamp. Then, it is brought into contact with the sensor surface. By this way, a thin polymer film is formed on the sensor surface via UV polymerization. When the template is removed from the surface, specific protein recognition sites are formed at the surface of the imprinted support [41–43]. There are a lot of significant advantages of the technique over conventional methods. Since this method is based on the imprinting of the protein onto a support, it reduces activity loss of the biorecognition molecule on the sensor surface. Thus it ensures long-term stability [44]. Only a very small amount of template molecule is enough for the imprinting and it does not require the protein to be in contact with the monomer solution prior to polymerization, which is very important for the conformational stability of the protein [45]. In the study, after modification of the gold surface with poly-tyramine and acryloyl chloride, the protein stamp was brought into contact with the capacitive electrode and PSA imprints were introduced onto the sensor surface. At the same time, electrodes with immobilized Anti-PSA antibodies (Anti-PSA electrodes) were prepared via glutaraldehyde activation, to compare the detection performances and selectivities of two methods. PSA detection studies were performed using standard PSA aqueous solutions. Selectivity of electrodes was tested against other proteins – human serum albumin (HSA) and human gamma globulin (IgG). Selectivity coefficients were calculated. PSA detection was also carried out from diluted human serum samples with the prepared electrodes. As the final step, reproducibility of the electrodes was tested.

## 2. Materials and methods

### 2.1. Materials

Prostate specific antigen (PSA, cat. no. A01238H) was obtained from Meridian Life Science, Inc., Memphis, USA. Anti-PSA antibody (cat. no. sc-7316) was obtained from Santa Cruz Biotechnology, Inc., Texas, USA. Human serum albumin (HSA) and tyramine (99%, $HOC_6H_4CH_2CH_2NH_2$) were obtained from Sigma (Steinheim, Germany). Human gamma globulin (human IgG) was purchased from Octapharma AB (Stockholm, Sweden). Acryloyl chloride and 1-dodecanethiol were obtained from Aldrich (Deisenhofen, Germany). Glutaraldehyde 50% (w/v), triethylamine, 3-amino-propyl-triethoxysilane (APTES) and α-α′-azoisobutyronitrile (AIBN) were purchased from Fluka (Buchs, Switzerland). Methacrylic acid (MAA) and ethylene glycol dimethacrylate (EGDMA) were obtained from Aldrich (Steinheim-Germany and USA, respectively). Glass microscope cover slips (24 × 40 mm) (Menzel-Glaser) were used as the base for protein stamp in microcontact imprinting. All other chemicals used were of analytical grade. All buffers were prepared with water treated with a reverse osmosis step with a Milli-Q system from Millipore (Bedford, MA, USA). This water was used

Please cite this article in press as: G. Ertürk, et al., Real-time prostate-specific antigen detection with prostate-specific antigen imprinted capacitive biosensors, Analytica Chimica Acta (2015), http://dx.doi.org/10.1016/j.aca.2015.07.055

all through the experiments if nothing else is stated. Prior to use, all buffers were filtered through a Millipore filter (pore size 0.22 μm) and degassed for 1 h.

### 2.2. Preparation of the microcontact-imprinted prostate specific antigen (PSA) capacitive electrodes (PSA-MIP)

The PSA-MIP capacitive sensor was developed in three steps as described below:

In the first step, glass cover slips (24 × 40 mm), which were used as protein stamps, were prepared. Cover slips were cleaned in 10 mL of 1 M HCl, de-ionized water, 1 M NaOH, de-ionized water and ethanol, respectively for 10 min in each step. After cleaning, they were dried with nitrogen gas. The cleaned cover slips were immersed in 10% (V/V) APTES (3-amino-propyl-triethoxysilane) in ethanol at room temperature for 1 h. By this way, the amino groups were introduced on the surface. After rinsing the surface with ethanol, the cover slips were immersed in 5% (V/V) glutaraldehyde (GA) solution in 10 mM phosphate buffer (pH 7.4) at room temperature for 2 h for the activation of amino groups. Then, they were rinsed with phosphate buffer and dried with nitrogen gas. For the immobilization of PSA onto the surface, the cover slips were immersed in 0.1 mg $mL^{-1}$ PSA solution (in 10 mM phosphate buffer, pH 7.4) at 4 °C for 24 h. Finally, they were washed with phosphate buffer and then dried with pure nitrogen gas.

In the second step, capacitive gold electrodes were subsequently cleaned with ethanol, de-ionized water, acetone, de-ionized water and acidic Piranha solution (3:1, $H_2SO_4$:$H_2O_2$, V/V) respectively for 10 min in each step. After plasma cleaning (Mod. PDC-3XG, Harrick, NY, USA) for 30 min, electropolymerization of tyramine was performed as described before [24], by cyclic voltammetry (CV) in ethanolic solution of 10 mM tyramine with a set potential range of 0–1.5 V (vs Ag/AgCl) and a scan rate of 50 mV $s^{-1}$ for 15 scans. By this way, free primary amino groups were introduced on the surface of the electrode. For the modification of the surface after tyramine electropolymerization, the electrodes were immersed in a solution containing 30 mM acryloyl chloride and 30 mM triethylamine (in toluene) overnight, at room temperature. Thus, the amide groups, which would interact with the protein stamp, were generated on the surface.

As the final step, before bringing the protein stamp into contact with the modified capacitive electrodes, monomer solution containing MAA as the functional monomer and EGDMA as the cross-linker were prepared in the ratio of 1:5 (V/V) and AIBN as the initiator was added into this solution. 1.5 μL of monomer solution was pipetted onto the electrode surface and the protein stamp (glass cover slip) was brought into contact with the electrode. The polymerization was initiated under UV light (365 nm, 400 W) and continued for 15 min. Then, the protein stamp was removed from the surface. Finally, the electrodes were immersed in 10 mM 1-dodecanethiol in ethanol for 20 min in order to block any pinholes in the polymer layer coating the electrode surface. The schematic representation of microcontact imprinting procedure is shown in Fig. 1.

### 2.3. Preparation of capacitive electrodes with immobilized anti-PSA antibody (Anti-PSA)

Capacitive electrodes with immobilized anti-PSA antibody (Anti-PSA) were prepared in three steps as described below:

In the first step, the electrodes were cleaned with the same chemicals used for PSA-MIP electrodes. After plasma cleaning for 30 min, electropolymerization of tyramine was performed as described in Section 2.2. Then the electrodes were rinsed with distilled water and dried with nitrogen gas.

In the second step, the electrodes were immersed in 5.0% (V/V) glutaraldehyde in 10 mM phosphate buffer (pH 7.4) for 1 h at room temperature. Then, they were thoroughly rinsed with phosphate buffer and dried with nitrogen gas. By this way, the amino groups on the surface of the electrode are modified by coupling to one of the aldehyde groups of glutaraldehyde leaving one free aldehyde group.

As the last step, the electrodes were kept in Anti-PSA solution (200 μg $mL^{-1}$) prepared in 10 mM phosphate buffer (pH 7.4) overnight at 4 °C. Finally, the electrodes were immersed in 1-dodecanethiol (10 mM) in ethanol for 20 min in order to cover bare parts of the gold surface.

### 2.4. Surface characterization of PSA-MIP electrodes

#### 2.4.1. Atomic force microscopy studies

In order to characterize the surface of the bare gold electrodes and PSA-MIP capacitive electrodes, atomic force microscope (AFM) was used in tapping mode (Nanomagnetics Instrument, Oxford, UK). Capacitive electrodes were attached on a sample holder by using double-sided carbon strips. Oscillation frequency (341.30 Hz), vibration amplitude (1 $V_{RMS}$) and free vibration amplitude (2 $V_{RMS}$) were used as experimental parameters. Imaging studies were made in 2 μm/s scanning rate and 256×256 pixels resolution.

#### 2.4.2. SEM images

The surface morphology of PSA-MIP electrode was observed by Scanning Electron Microscope (SEM, FEI, Quanta 200 FEG, USA). The electrodes were washed with ethanol and water for 10 min, respectively. Before SEM observation, the electrodes were sputter coated with Au/Pd.

#### 2.4.3. Cyclic voltammetry (CV) studies

CV experiments were carried out using a potentiostat/galvanostat (Autolab PGSTAT12, EcoChemie, Utrecht, The Netherlands). Instrument operation and data acquisition were controlled using GPES 4.8 Software. All electrochemical measurements were conducted in a standard three-electrode flow cell fitted with a platinum wire and a commercial Ag/AgCl electrode as the counter and the reference electrodes, respectively. The PSA-MIP and Anti-PSA gold electrodes, during the different steps of their preparation, served as the working electrodes. A solution of KCl (0.1 M) containing 0.1 M potassium ferricyanide was used as the electrolyte solution. Cyclic voltammetry was performed by sweeping the potential between −0.3 and 0.8 V at a sweep rate of 0.1 V $s^{-1}$.

### 2.5. Capacitive measurements with PSA-MIP and Anti-PSA electrodes

The capacitive measurements have been performed with an automated flow-injection system (CapSenze HB, Lund, Sweden). The capacitive electrode was inserted in the electrochemical flow cell and connected to the platinum auxiliary and reference electrodes. The capacitance measurement was performed via a current pulse method, as previously described [23]. The theory of current pulse technique is based on the principle of an electrical double layer and the electrode–solution interface is based on an assumption that the system could be described as a simple resistor–capacitor circuit model. Current pulse technique offers some advantages over the potential pulse technique. In the technique, the use of microampere constant current is more favorable for the electrodes to be resistant against external electronic disturbances which can lead to inaccurate measurement and poor baseline stability. The calculation of capacitance does not depend on the resistance value and the calculation is done in a simple and

Please cite this article in press as: G. Ertürk, et al., Real-time prostate-specific antigen detection with prostate-specific antigen imprinted capacitive biosensors, Analytica Chimica Acta (2015), http://dx.doi.org/10.1016/j.aca.2015.07.055

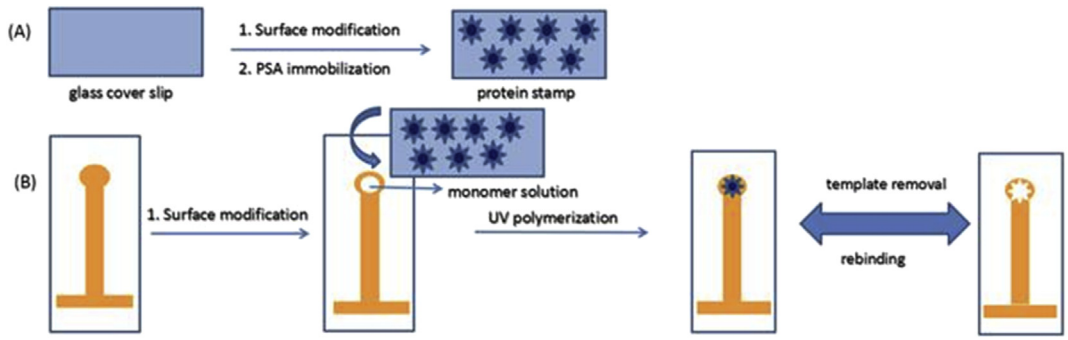


**Fig. 1.** Schematic representation of the microcontact imprinting of PSA onto the capacitive biosensor. (A) Preparation of the glass cover slips (protein stamps), (B) Preparation of the capacitive gold electrodes and microcontact imprinting via UV polymerization.

accurate way because of the linearity of potential response to the pulse of current. Four values of capacitance are calculated from one cycle of current supply. Thus, a higher accuracy is obtained. The analysis are completed in a shorter time period compared to existing methods; wherein the resistance has to be calculated in the first step, then the capacitance is determined by a logarithmic equation. Due to this, different steps will prolong the analysis time and lead to a higher inaccuracy of the capacitance measurements. (Detailed information about current pulse method can be found in Supplementary Information).

In the first step, a regeneration solution (25 mM glycine-HCl, pH 2.5) was injected into the system to regenerate the surface. This step was repeated between each analyte injection. After injection of running buffer to get a stable baseline, the standard solutions of different concentrations of PSA (10 fg $mL^{-1}$–100 ng $mL^{-1}$) were injected sequentially. The binding of the target protein (PSA) to the electrode surface resulted in a decrease of the registered capacitance and the change was calculated automatically by CapSenze Smart Software (CSS). In all of the analyses, the flow rate was 100 μL $min^{-1}$ and the injected sample volume was 250 μL.

In order to evaluate the selectivity of the electrodes prepared by two different methods, the responses of the capacitive system against the other proteins – HSA and IgG were monitored. HSA and IgG solutions were applied in singular manner and also in competitive manner. The protein concentration was 1.0 ng $mL^{-1}$ for each protein during analysis.

Real sample analysis was carried out on serum from healthy humans. For this purpose, the blood sample was taken into test tubes and then, centrifuged at 3300× g at room temperature for 10 min. Later on, the samples were passed from a filter with pore sizes of 3 μm and stored in a deep freeze at −20 °C until use. The collected healthy human serum samples were diluted with 10 mM phosphate buffer (pH 7.4). Samples, in which PSA could not be detected, were selected as blank samples. The other samples were obtained by spiking standard PSA solution in blank human serum, and then used for the analysis.

For the determination of reusability of the capacitive electrodes, PSA was detected repeatedly, using the assay cycle regeneration–equilibration–injection, with PSA-MIP and Anti-PSA electrodes. Reproducibility of the assays was evaluated by monitoring the change in capacitance at repeated assays at the same concentration of PSA, 1.0 ng $mL^{-1}$.

## 3. Results and discussion

### 3.1. Surface characterization of PSA-MIP capacitive electrodes

Surface characterization of PSA-MIP electrode was determined by AFM, SEM and cyclic voltammetry.

AFM images of the bare surface and PSA-MIP electrode are shown in Fig. 2A and B, respectively. As clearly seen from the figures, due to the polymerization process, a rough polymeric surface was formed on the gold electrode. The surface deepness of the electrode was increased from 6.90 nm, the surface deepness of bare gold surface, to 232 nm determined by AFM measurements.

SEM images in Fig. 2C and D also show the polymeric surface on the PSA-MIP electrode in different magnifications (3.00× and 5.00×).

Proper insulation of the electrode surface is crucial for the design of capacitive biosensors [20–25]. Hence, defects in the layer covering the gold electrode surface can allow the contacting solution to reach the electrode surface and thus to increase the level of capacitance due to the high polarity of water. Cyclic voltammetry is a valuable method to detect the degree of insulation of the electrode surface [20–27]. Cyclic voltammogram of PSA-MIP capacitive electrode is shown in Fig. 2E (CV characterization of Anti-PSA capacitive electrode is shown in Supplementary Information, Fig. SI 1). The redox couple was oxidized and reduced during cycling of potential between −0.3 and 0.8 V at a scan rate of 0.1 V $s^{-1}$ at the clean gold surface according to the curves in Fig. 2E. The redox peaks decreased after each layer. Finally, treatment with 1-dodecanethiol reduced the redox currents substantially as seen from the disappearance of the redox peaks in curve c in Fig. 2E. The CV results show that the surfaces of the electrodes are insulated well and they can be used in the subsequent capacitive measurements.

### 3.2. Capacitive measurements with PSA-MIP and Anti-PSA electrodes

PSA-MIP capacitive electrode was placed in the electrochemical flow cell and it was connected to an automated flow-injection system. 10 mM phosphate (pH 7.4) was used as the running buffer which was continuously pumped through the flow system at a flow rate of 100 μL $min^{-1}$. PSA solutions containing different concentrations of PSA (10 fg $mL^{-1}$–10 ng $mL^{-1}$) were prepared in the running buffer and sequentially injected into the capacitive system. Each solution was injected for 3 times. After injection and equilibration period in totally 15 min, regeneration buffer, 25 mM glycine-HCl (pH 2.5), was injected to regenerate the system during 2.5 min. After waiting 45 min for reconditioning and re-equilibration of the system, a second injection period started (Supplementary Information, Fig. SI 2). The capacitance graphs were obtained by plotting the capacitance change (−nF $cm^{-2}$) versus the logarithm of PSA concentrations (ng $mL^{-1}$). In order to obtain a reliable analytical signal, an average of the last five

Please cite this article in press as: G. Ertürk, et al., Real-time prostate-specific antigen detection with prostate-specific antigen imprinted capacitive biosensors, Analytica Chimica Acta (2015), http://dx.doi.org/10.1016/j.aca.2015.07.055

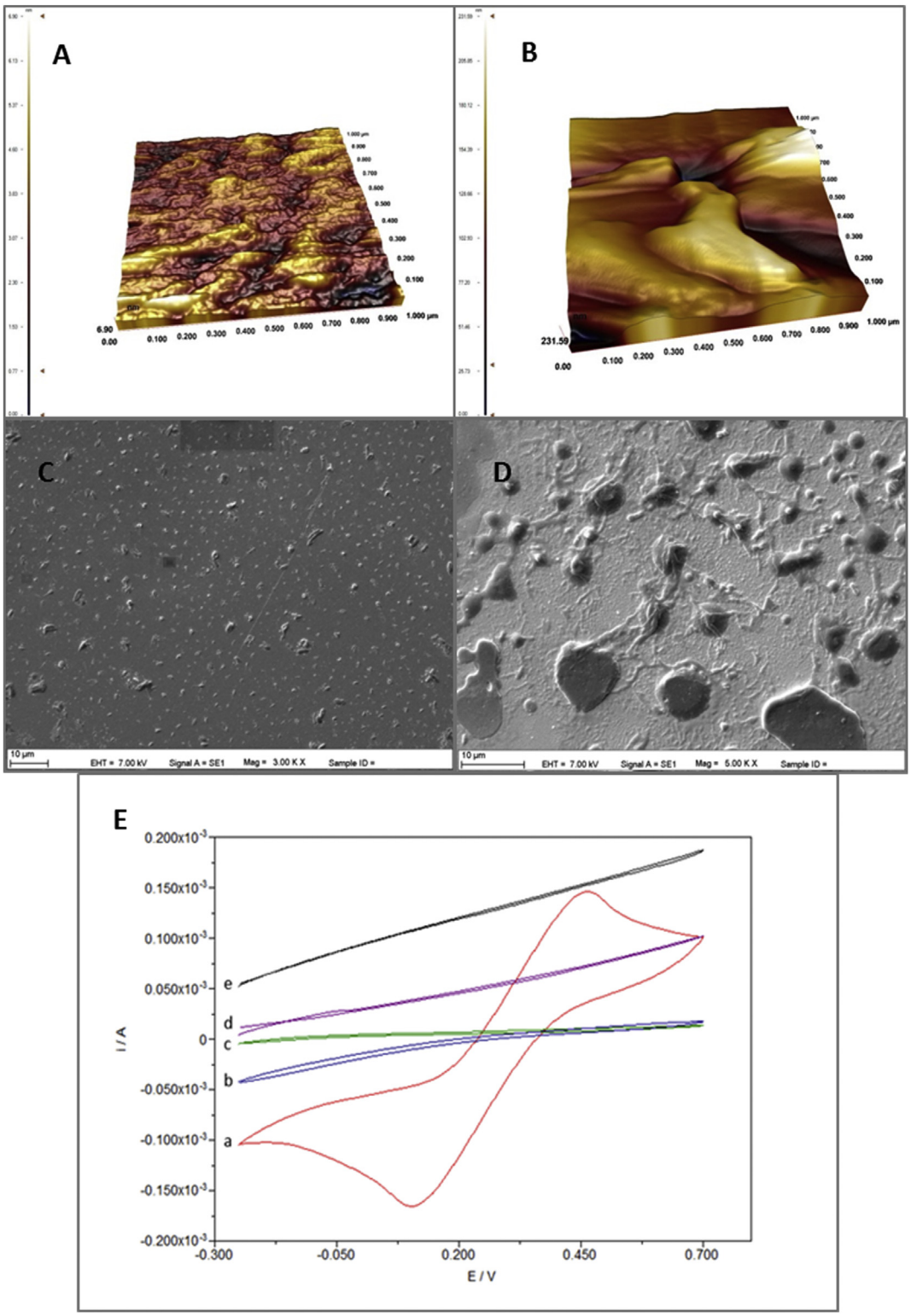


**Fig. 2.** Characterization of electrodes; (A) AFM image of bare gold surface, (B) AFM image of PSA-MIP electrode, (C–D) SEM images of PSA-MIP electrode, (E) Cyclic voltammogram recorded in a solution of 100 mM KCl containing 100 mM $K_3[Fe(CN)_6]$ using: bare electrode (red-a), gold electrode after electropolymerization of tyramine (black-e), gold electrode after surface modification with acryloyl chloride (purple-d), gold electrode after UV polymerization (blue-b), gold electrode after treatment with 1-dodecanethiol (green-c). The scan range was from −0.3 to 0.8 V (vs. Ag/AgCl), at a scan rate of 0.1 V $s^{-1}$. (For interpretation of the references to color in this figure legend, the reader is referred to the web version of this article.)

capacitance readings was calculated. Fig. 3A shows the 15 min injection and equilibration period after injection of standard PSA solutions in the concentration range of 10 fg $mL^{-1}$ and 10 ng $mL^{-1}$. As seen from Fig. 3A, the decrease in capacitance increased with the increasing PSA concentrations. The binding of PSA to the electrode surface resulted in a decrease of the registered capacitance.

Please cite this article in press as: G. Ertürk, et al., Real-time prostate-specific antigen detection with prostate-specific antigen imprinted capacitive biosensors, Analytica Chimica Acta (2015), http://dx.doi.org/10.1016/j.aca.2015.07.055

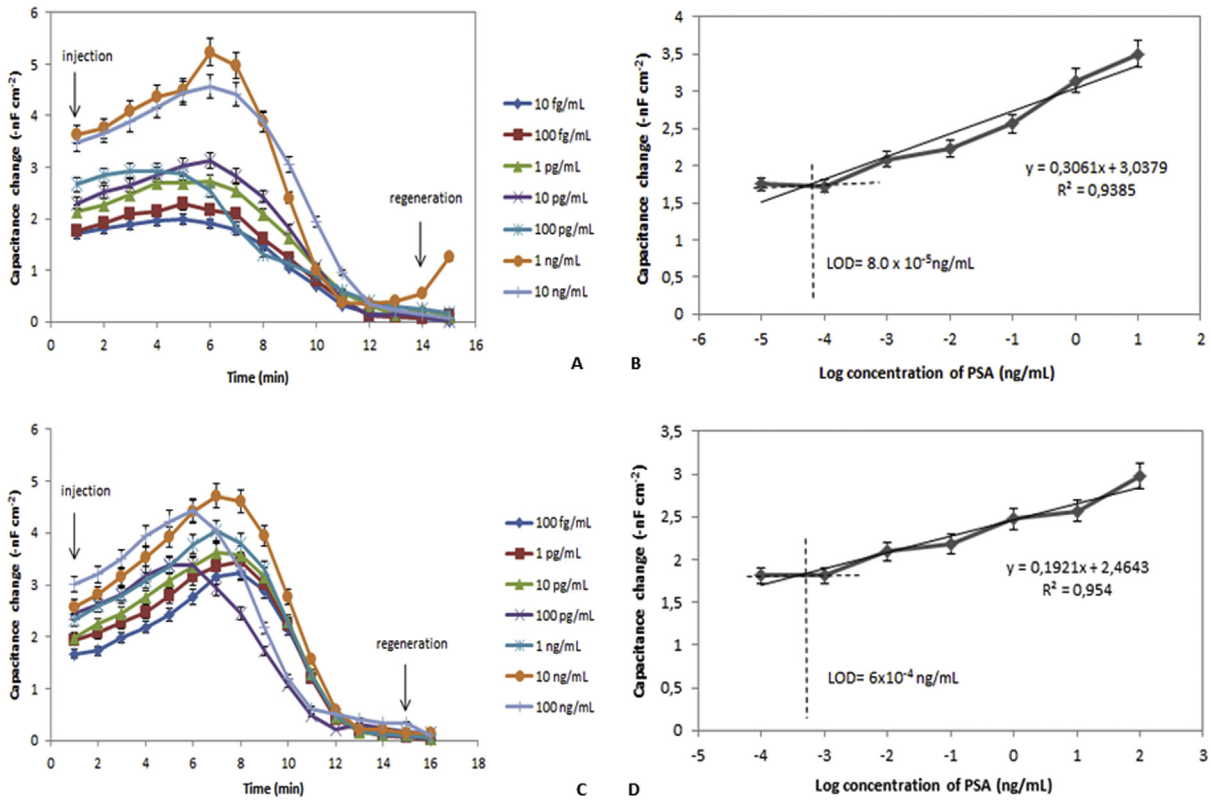


**Fig. 3.** A) Capacitance change of the PSA-MIP electrode vs. PSA concentrations under optimum conditions, B) Calibration curve for PSA detection measured with PSA-MIP capacitive biosensor under optimum conditions, C) Capacitance change of the Anti-PSA electrode vs. PSA concentrations under optimum conditions, D) Calibration curve for PSA detection measured with Anti-PSA capacitive biosensor under optimum conditions (Flow rate 100 μL $min^{-1}$; sample volume 250 μL; running buffer 10 mM phosphate, pH 7.4; regeneration buffer 25 mM glycine-HCl, pH 2.5; T 25 °C).

CapSenze Smart Software was used to automatically calculate the change in capacitance. As seen from Fig. 3A, when the PSA solution was injected to the system, the capacitance started to decrease in 5 min and came to an equilibrium in 10 min. Thus, the injection and equilibration period continued for 15 min. Then, a 45 min regeneration period was started (Actual sensogram is shown in Supplementary Information, Fig. SI-2). The calibration graph that shows the capacitance change vs. log concentration of PSA (ng $mL^{-1}$) is shown in Fig. 3B. The graph was drawn from the data spots in Fig. 3A. The capacitance change (Y-axis) in Fig. 3B was estimated from the capacitance change (Y-axis) in Fig. 3A. A linear relationship was obtained between $1.0 \times 10^{-4}$ and $1.0 \times 10^{1}$ ng $mL^{-1}$ and the limit of detection (LOD) was determined to be $8.0 \times 10^{-5}$ ng $mL^{-1}$ (Fig. 3B), based on IUPAC guidelines [46]. The capacitance change in the studied concentration range was linear with the regression equation of $y = 0.3061x + 3.0379$ ($R^2 = 0.9385$).

Anti-PSA electrode was also tested for PSA detection. The regeneration and running buffers were the same as the buffers for PSA-MIP electrode. The conditions for the analysis were exactly the same as the conditions for PSA-MIP electrode. PSA solutions containing different concentrations of PSA (100 fg $mL^{-1}$–100 ng $mL^{-1}$) were prepared in the running buffer and injected into the system for three times. Fig. 3C shows the 15 min injection and equilibration period. As seen from Fig. 3C, the decrease in capacitance increased with the increasing PSA concentrations and a linear relationship was obtained between $1.0 \times 10^{-3}$ and $1.0 \times 10^{2}$ ng $mL^{-1}$. The LOD was determined to be $6.0 \times 10^{-4}$ ng $mL^{-1}$ (Fig. 3D), based on IUPAC guidelines [46]. The capacitance change in the studied concentration range was linear with the regression equation of $y = 0.1921x + 2.4643$ ($R^2 = 0.954$).

The analytical performances reported in literature of different biosensors used for PSA detection are shown in Table 1. The LOD value of PSA-MIP electrode in this study is much lower than that of the other methods.

### 3.3. Selectivity of the PSA-MIP and Anti-PSA electrodes against competing proteins

In order to test the selectivity of the PSA-MIP and Anti-PSA electrodes, HSA and IgG were used as the competing proteins, as has been done in many earlier studies on PSA detection [47–61]. IgG and HSA are the dominating proteins in human serum. They are found in the levels of mg $mL^{-1}$ where PSA is normally found as 4.0 ng $mL^{-1}$ in human serum. It is important to show the selectivity of the developed sensor against proteins of 1-million fold higher concentrations especially to test the applicability of the developed sensor for clinical applications. For this purpose, aqueous solutions of PSA, HSA and IgG proteins were injected into the system in singular manner. Also, pre-mixed solutions having PSA/HSA, PSA/IgG and PSA/HSA/IgG were injected into the system to test the competitive binding between the different proteins and PSA. Standard protein solutions were prepared in the running buffer and the concentration was 1.0 ng $mL^{-1}$ for each of them. The molar concentrations of the proteins used in the selectivity experiments were: PSA ($0.61 \times 10^{-10}$ M), HSA ($1.20 \times 10^{-10}$ M) and IgG ($2.71 \times 10^{-10}$ M).

As seen from Fig. 4A, the change in capacitance was very low for the standard HSA and IgG solutions compared to that for PSA for the capacitive electrodes. Pre-mixed protein solutions caused a lower

Please cite this article in press as: G. Ertürk, et al., Real-time prostate-specific antigen detection with prostate-specific antigen imprinted capacitive biosensors, Analytica Chimica Acta (2015), http://dx.doi.org/10.1016/j.aca.2015.07.055

**Table 1**
Comparison of analytical performances of different techniques used for PSA detection.

| Method | Detection limit | Reference |
|---|---|---|
| Potentiometric immunosensor | 0.04 ng $mL^{-1}$ | [47] |
| Impedimetric immunosensor | $0.73 \times 10^{-3}$ ng $mL^{-1}$ | [48] |
| Electrochemical immunosensor | 0.5 ng $mL^{-1}$ | [49] |
| Fluorescent immunosensor | $0.1 \times 10^{-3}$ ng $mL^{-1}$ | [50] |
| Electrogenerated chemiluminescence peptide-based biosensor | $8 \times 10^{-7}$ ng $mL^{-1}$ | [51] |
| Dark field microscopy | $4.5 \times 10^{-7}$ ng $mL^{-1}$ | [52] |
| Chemiluminescent aptasensors | 0.5 ng $mL^{-1}$ | [53] |
| Microfabricated tin-film electrochemical sensor | 0.12 ng $mL^{-1}$ | [54] |
| Electrochemical Impedance Spectroscopy (EIS) | 1 ng $mL^{-1}$ | [55] |
| Suspension array technology | 0.047 ng $mL^{-1}$ | [56] |
| Electrochemical immunosensor | $1 \times 10^{-3}$ ng $mL^{-1}$ | [57] |
| Electrochemiluminescence Immunoassay | $0.3 \times 10^{-3}$ ng $mL^{-1}$ | [58] |
| Capacitive immunosensor | 3 ng $mL^{-1}$ | [59] |
| Electrochemical immunosensor | $0.6 \times 10^{-3}$ ng $mL^{-1}$ | [60] |
| Field-effect transistor (FET) biosensor | $1.0 \times 10^{-4}$ ng $mL^{-1}$ | [61] |
| Microcontact-PSA Imprinted capacitive biosensor | $8.0 \times 10^{-5}$ ng $mL^{-1}$ | In this study |

capacitance change compared to the standard PSA solution. The difference could be stemmed from the competitive effects of the other proteins. However, the electrodes could detect PSA in singular manner and also under competitive conditions.

The results obtained from PSA-MIP electrode are similar to the results obtained from the Anti-PSA electrode. The selectivity coefficients (k) were calculated as $\Delta C_{PSA}/\Delta C_{competitor}$. Relative selectivity coefficient was calculated as $k_{PSA\text{-}MIP}/k_{Anti\text{-}PSA}$ for HSA and IgG, respectively. The calculated selectivity coefficients for the two electrodes are shown in Fig. 4B. According to the selectivity coefficients calculated for PSA versus HSA, PSA-MIP electrode is more selective for PSA than Anti-PSA electrode. On the other hand, there is not a big difference for the selectivity coefficients of two electrodes for IgG. However, relative selectivity coefficients show that the PSA-MIP electrode could detect PSA with a higher sensitivity than what could be achieved with the Anti-PSA electrode. It is important to emphasize that, in these experiments, the selectivity and specificity of the MIP system was compared with the Anti-PSA antibody immobilized system. Antibody immobilization is a powerful and frequently used technique for the design of biosensors. The relative selectivity coefficients (k′) of 2.06 for HSA and 0.84 for IgG may be lower selectivity values when the MIP system is compared with the NIP system. However, in our study, these values indicate high selectivity and sensitivity since the MIP system was

**Table 2**
Recovery tests for PSA spiked in human serum samples (n = 3).

| Samples | Added PSA (pg/mL) | Found PSA (pg/mL) | Recovery (%) |
|---|---|---|---|
| Human serum 1 | 0.1 | 0.12 ± 0.05 | 120 |
| Human serum 2 | 1 | 0.9 ± 0.3 | 90 |
| Human serum 3 | 10 | 10.8 ± 0.2 | 108 |
| Human serum 4 | 100 | 103 ± 0.1 | 103 |

A

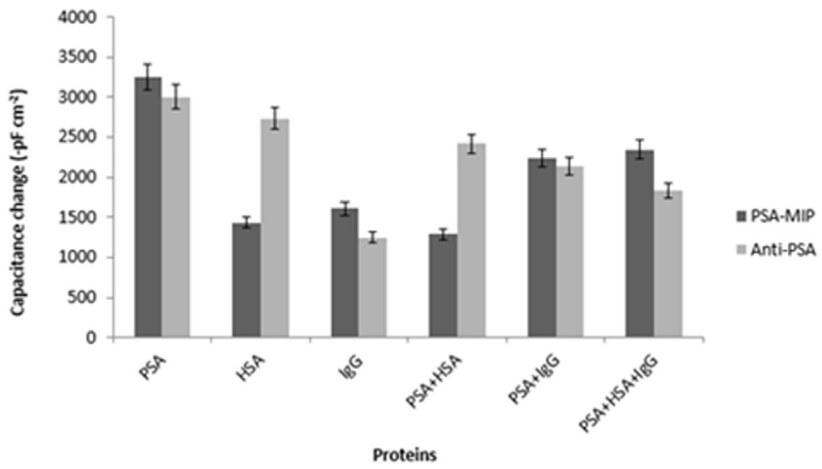


B

| Protein | ΔC (pF) PSA-MIP | ΔC (pF) Anti-PSA | Selectivity coeff (k) PSA-MIP | Selectivity coeff (k) Anti-PSA | Rel. selectivity coeff (k′) |
|---|---|---|---|---|---|
| PSA | 3250 | 3000 | - | - | - |
| HSA | 1433 | 2730 | 2.27 | 1.10 | 2.06 |
| IgG | 1608 | 1250 | 2.02 | 2.40 | 0.84 |

**Fig. 4.** A) Selectivity of PSA-MIP and Anti-PSA capacitive biosensors against competitor proteins; HSA (human serum albumin) and IgG (immunoglobulin G) in singular and competitive manner (protein concentration 1.0 ng $mL^{-1}$; flow rate 100 μL $min^{-1}$; sample volume 250 μL; running buffer 10 mM phosphate, pH 7.4; regeneration buffer 25 mM glycine-HCl, pH 2.5; T 25 °C), B) Selectivity coefficients of PSA-MIP and Anti-PSA electrodes [Δ: Capacitance change for the PSA-MIP and Anti-PSA electrodes, k: selectivity coefficient for PSA versus competing proteins, k′: relative selectivity coefficient for PSA-MIP electrode versus Anti-PSA electrode].

Please cite this article in press as: G. Ertürk, et al., Real-time prostate-specific antigen detection with prostate-specific antigen imprinted capacitive biosensors, Analytica Chimica Acta (2015), http://dx.doi.org/10.1016/j.aca.2015.07.055

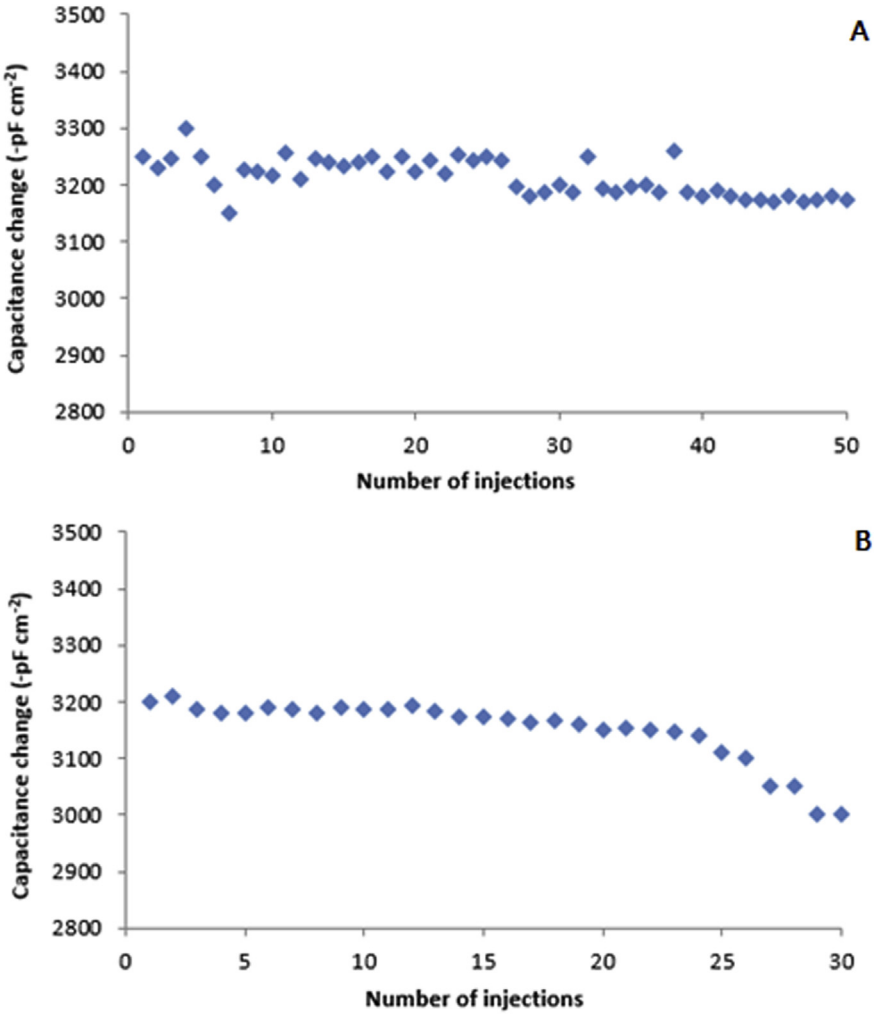


**Fig. 5.** A) Reproducibility of the PSA-MIP capacitive biosensor (PSA concentration 1,0 ng $mL^{-1}$; flow rate 100 μL $min^{-1}$; sample volume 250 μL; running buffer 10 mM phosphate, pH 7.4; regeneration buffer 25 mM glycine-HCl, pH 2.5; T 25 °C), B) Reproducibility of the Anti-PSA capacitive biosensor (PSA concentration 1,0 ng $mL^{-1}$; flow rate 100 μL $min^{-1}$; sample volume 250 μL; running buffer 10 mM phosphate, pH 7.4; regeneration buffer 25 mM glycine-HCl, pH 2.5; T 25 °C).

compared with a powerful antibody immobilization technique, which is based on antigen–antibody interaction.

### 3.4. PSA detection from human serum

In order to investigate the applicability and reliability of the PSA-MIP capacitive biosensors for clinical applications, recovery experiments were performed by detection of PSA spiked in human serum samples. The results are shown in Table 2. A recovery was obtained in the range of 90% and 120% for PSA-MIP electrode. Serum contains a large number of biological substances like enzymes, hormones, antibodies etc. PSA detection on the fg $mL^{-1}$ level is a successful result since undiluted serum sample or other biological substances have a 1-million fold higher PSA concentration. Therefore, this detection limit indicates high detection sensitivity.

### 3.5. Reproducibility

The PSA-MIP and Anti-PSA electrodes were evaluated in terms of reproducibility by monitoring the capacitance change ($-$pF $cm^{-2}$) at the same concentration of standard PSA solution (1.0 ng $mL^{-1}$). After injection and equilibration periods, in total 15 min, regeneration buffer was injected during 2.5 min before running buffer was used for reconditioning until a stable baseline signal was achieved. The capacitance changes of the PSA-MIP and Anti-PSA electrodes versus the number of injections are shown in Fig. 5A and B, respectively.

The PSA detection activity of the PSA-MIP electrode retained about the same level during 50 injections. Microcontact imprinting method has an advantage of reducing activity loss of the template molecule during the application [40–43,62]. The same PSA-MIP electrode was used in whole experiments and triplicate measurements were made for each analysis. This is a promising result as hence, the PSA-MIP electrodes can be reused for PSA detection with good reproducibility without significant loss in activity.

On the other hand, the same results could not be observed for Anti-PSA electrode. In Fig. 5B, it can be clearly seen that the electrode started to lose its activity after 25 injections. The most important difference between the two methods, the microcontact imprinting and the antibody immobilization technique, is the ongoing detection performance of the microcontact-imprinted electrodes.

## 4. Conclusion

In this study, a capacitive immunosensor was developed for real-time, selective and sensitive detection of PSA with two

Please cite this article in press as: G. Ertürk, et al., Real-time prostate-specific antigen detection with prostate-specific antigen imprinted capacitive biosensors, Analytica Chimica Acta (2015), http://dx.doi.org/10.1016/j.aca.2015.07.055

different methods: microcontact imprinting of PSA and anti-PSA antibody immobilization. PSA detection performances of the electrodes prepared with the following methods were compared. The electrode which was prepared with the microcontact imprinting was better in detection, selectivity and reproducibility. The microcontact imprinting method does not require the protein to be present in the monomer solution prior to polymerization, only a small amount of template protein is required for the imprinting process and this method has successful applications with the macromolecular templates, like proteins. When advantages of the capacitive immunosensor technology are combined with the advantages of the microcontact imprinting method, the resulting system is very promising for the detection of biomarkers important for diagnosis of various diseases in a rapid, highly sensitive and selective manner.

## Acknowledgments

GE was supported by a fellowship by Hacettepe University, Turkey.

The project was also supported by the Swedish Research Council and the instrument used for analysis was a loan from CapSenze HB, Lund, Sweden.

## Appendix A. Supplementary information

Supplementary data related to this article can be found at http://dx.doi.org/10.1016/j.aca.2015.07.055.

## References

[1] H. Özen, S. Sözen, PSA isoforms in prostate cancer detection, Eur. Urol. Suppl. 5 (2006) 495–499.
[2] F. Saad, The treatment continuum in the management of prostate cancer patients: what's new? Eur. Urol. Suppl. 5 (2006) 539–542.
[3] H. Grönberg, Prostate cancer epidemiology, Lancet 361 (2003) 859–864.
[4] R. Etzioni, N. Urban, S. Ramsey, M. McIntosh, S. Schwartz, B. Reid, J. Radich, G. Anderson, L. Hartwell, Early detection: the case for early detection, Nat. Rev. Cancer 3 (2003) 243–252.
[5] L. Huang, G. Reekmans, D. Saerens, J.-M. Friedt, F. Frederix, L. Francis, S. Muyldermans, A. Campitelli, C.V. Hoof, Prostate-specific antigen immunosensing based on mixed self-assembled monolayers, camel antibodies and colloidal gold enhanced sandwich assays, Biosens. Bioelectron. 21 (2005) 483–490.
[6] R.A. Bok, E.J. Small, Bloodborne biomolecular markers in prostate cancer development and progression, Nat. Rev. Cancer 2 (2002) 918–926.
[7] R.B. Nadler, P.A. Humphrey, D.S. Smith, W.J. Catalona, T.L. Ratliff, Effect of inflammation and benign prostatic hyperplasia on elevated serum prostate specific antigen levels, J. Urol. 154 (1995) 407–413.
[8] M.C. Benson, I.S. Whang, A. Pantuck, K. Ring, S.A. Kaplan, C.A. Olsson, W.H. Cooner, Prostate specific antigen density: a means of distinguishing benign prostatic hypertrophy and prostate cancer, J. Urol. 147 (192) 815–816.
[9] U.H. Stenmann, J. Leinonen, W.-M. Zhang, P. Finne, Prostate-specific antigen, Semin. Cancer Biol. 9 (1999) 83–93.
[10] H.J. Linton, L.S. Marks, L.S. Millar, C.L. Knott, H.G. Rittenhouse, S.D. Mikolajczyk, Benign prostate-specific antigen (BPSA) in serum is increased in benign prostate disease, Clin. Chem. 49 (2003) 253–259.
[11] A.H. Declan, C.J. Hayes, P. Leonard, L. McKenna, R. O'Kennedy, Biosensor developments: application to prostate-specific antigen detection, Trends Biotechnol. 25 (2007) 125–131.
[12] P. D'Orazio, Biosensors in clinical chemistry—2011 update, Clin. Chim. Acta 412 (2011) 1749–1761.
[13] A.C. Barton, F. Davis, S.P.J. Higson, Labeless immunosensor assay for prostate specific antigen with picogram per milliliter limits of detection based upon an ac impedance protocol, Anal. Chem. 80 (2008) 6198–6205.
[14] M.A. Bangar, D.J. Shirale, W. Chen, N.V. Myung, A. Mulchandani, Single conducting polymer nanowire chemiresistive label-free immunosensor for cancer biomarker, Anal. Chem. 81 (2009) 2168–2175.
[15] G. Robinson, The commercial development of planar optical biosensors, Sens. Actuators B 29 (1995) 31–36.
[16] T.M.H. Lee, Over-the-counter biosensors: past, present, and future, Sensors 8 (2008) 5535–5559.
[17] B. Mattiasson, K. Teeparuksapun, M. Hedström, Immunochemical binding assays for detection and quantification of trace impurities in biotechnological production, Trends Biotechnol. 28 (2009) 20–27.
[18] M. Steltze, E. Sackmann, Sensitive detection of protein adsorption to supported lipid bilayers by frequency-dependent capacitance measurements and microelectrophoresis, Biochim. Biophys. Acta 981 (1989) 135–142.
[19] C. Berggren, B. Bjarnason, G. Johansson, Capacitive biosensors, Electroanalysis 13 (2001) 173–180.
[20] W. Limbut, M. Hedström, P. Thavarungkul, P. Kanatharana, B. Mattiasson, Capacitive biosensor for detection of endotoxin, Anal. Bioanal. Chem. 389 (2007) 517–525.
[21] M. Labib, M. Hedström, M. Amin, B. Mattiasson, A multipurpose capacitive biosensor for assay and quality control of human immunoglobulin G, Biotechnol. Bioeng. 104 (2009) 312–320.
[22] M. Hedström, I.Y. Galaev, B. Mattiasson, Continuous measurements of a binding reaction using a capacitive biosensor, Biosens. Bioelectron. 21 (2005) 41–48.
[23] D. Erlandsson, K. Teeparuksapun, B. Mattiasson, M. Hedström, Automated flow-injection immunosensor based on current pulse capacitive measurements, Sensors Actuators B 190 (2014) 295–304.
[24] K. Teeparuksapun, M. Hedström, E.Y. Wong, S. Tang, I.K. Hewlett, B. Mattiasson, Ultrasensitive detection of HIV-1 p24 antigen using nanofunctionalized surfaces in a capacitive immunosensor, Anal. Chem. 82 (2010) 8406–8411.
[25] M. Labib, M. Hedström, M. Amin, B. Mattiasson, A capacitive biosensor for detection of staphylococcal enterotoxin B, Anal. Bioanal. Chem. 393 (2009) 1539–1544.
[26] M. Labib, M. Hedström, M. Amin, B. Mattiasson, A novel competitive capacitive glucose biosensor based on concanavalin A-labeled nanogold colloids assembled on a polytyramine-modified gold electrode, Anal. Chim. Acta 659 (2010) 194–200.
[27] L. Lebogang, B. Mattiasson, M. Hedström, Capacitive sensing of microcystin variants of *Microcystis aeruginosa* using a gold immunoelectrode modified with antibodies, gold nanoparticles and polytyramine, Microchim. Acta 181, 1009–1017.
[28] K. Haupt, Peer reviewed: molecularly imprinted polymers: the next generation, Anal. Chem. 1 (2003) 376–383.
[29] G. Wulff, A. Sarhan, K. Zabrocki, Enzyme-analogue built polymers and their use for the resolution of racemates, Tetrahedron Lett. 14 (1973) 4329–4332.
[30] G. Wulff, Enzyme-like catalysis by molecularly imprinted polymers, Chem. Rev. 102 (2002) 1–27.
[31] K. Haupt, Molecularly imprinted polymers in analytical chemistry, Analyst 126 (2001) 747–756.
[32] D.R. Kryscio, N.A. Peppas, Surface imprinted thin polymer film systems with selective recognition for bovine serum albumin, Anal. Chim. Acta 718 (2012) 109–115.
[33] N. Bergmann, N.A. Peppas, Molecularly imprinted polymers with specific recognition for macromolecules and proteins, Prog. Polym. Sci. 33 (2008) 271–288.
[34] G. Ertürk, L. Uzun, M.A. Tümer, R. Say, A. Denizli, Fab sub-fragments imprinted SPR biosensor for real-time human immunoglobulin G detection, Biosens. Bioelectron. 28 (2011) 97–104.
[35] G. Şener, E. Özgür, E. Yılmaz, L. Uzun, R. Say, A. Denizli, Quartz crystal microbalance based nanosensor for lysozyme detection with lysozyme imprinted nanoparticles, Biosens. Bioelectron. 26 (2010) 815–821.
[36] M. Andaç, I.Y. Galaev, A. Denizli, Dye attached poly (hydroxyethyl methacrylate) cryogel for albumin depletion from human serum, J. Sep. Sci. 35 (2012) 1173–1182.
[37] H.Y. Lin, C.Y. Hsu, J.L. Thomas, S.E. Wang, H.C. Chen, T.C. Chou, The microcontact imprinting of proteins: the effect of cross-linking monomers for lysozyme, ribonuclease A and myoglobin, Biosens. Bioelectron. 22 (2006) 534–543.
[38] P.C. Liao, Y.C. Tyan, C.Y. Wang, J.F. Hsu, T.C. Chou, H.Y. Lin, Assessing the binding selectivity of molecularly imprinted polymer artificial antibodies by mass spectrometry-based profiling system, J. Biomed. Mater. Res. A 91A (2009) 597–604.
[39] P.C. Chou, J. Rick, T.-C. Chou, C-reactive protein thin-film molecularly imprinted polymers formed using a micro-contact approach, Anal. Chim. Acta 542 (2005) 20–25.
[40] L. Chen, S. Xu, J. Li, Recent advances in molecular imprinting technology: current status, challenges and highlighted applications, Chem. Soc. Rev. 40 (2011) 2922–2942.
[41] G. Şener, E. Özgür, A.Y. Rad, L. Uzun, R. Say, A. Denizli, Rapid real-time detection of procalcitonin using a microcontact imprinted surface plasmon resonance biosensor, Analyst 138 (2013) 6422–6428.
[42] B. Osman, L. Uzun, N. Beşirli, A. Denizli, Microcontact imprinted surface plasmon resonance sensor for myoglobin detection, Mat. Sci. Eng. C 33 (2013) 3609–3614.
[43] C.Y. Hsu, H.Y. Lin, J.L. Thomas, T.C. Chou, Synthesis of and recognition by ribonuclease A imprinted polymers, Nanotechnology 17 (2006) 77–83.
[44] H.Y. Lin, J. Rick, T.C. Chou, Optimizing the formulation of a myoglobin molecularly imprinted thin-film polymer—formed using a micro-contact imprinting method, Biosens. Bioelectron. 22 (2007) 3293–3301.
[45] H.W. Chien, W.B. Tsai, Fabrication of tunable micropatterned substrates for cell patterning via microcontact printing of polydopamine with poly (ethylene imine)-grafted copolymers, Acta Biomater. 8 (2012) 3678–3686.
[46] R.P. Buck, E. Lindner, Recommendations for nomenclature of ionselective electrodes (IUPAC Recommendations 1994), Pure Appl. Chem. 66 (1994)

2527–2536.
[47] B. Zhang, B. Liu, G. Chen, D. Tang, Competitive-type displacement reaction for direct potentiometric detection of low-abundance protein, Biosens. Bioelectron. 53 (2014) 465–471.
[48] L. Hou, Z. Gao, M. Xu, X. Cao, X. Wu, G. Chen, D. Tang, DNAzyme-functionalized gold–palladium hybrid nanostructures for triple signal amplification of impedimetric immunosensor, Biosens. Bioelectron. 54 (2014) 365–371.
[49] B. Kavosi, A. Salimi, R. Hallaj, K. Amani, A highly sensitive prostate-specific antigen immunosensor based on gold nanoparticles/PAMAM dendrimer loaded on MWCNTS/chitosan/ionic liquid nanocomposite, Biosens. Bioelectron. 52 (2014) 20–28.
[50] Y. Zhu, J. Peng, L. Jiang, J. Zhu, Fluorescent immunosensor based on CuS nanoparticles for sensitive detection of cancer biomarker, Analyst 139 (2014) 649–655.
[51] H. Qi, M. Li, M. Dong, S. Ruan, Q. Gao, C. Zhang, Electrogenerated chemiluminescence peptide-based biosensor for the determination of prostate-specific antigen based on target-induced cleavage of peptide, Anal. Chem. 86 (2014) 1372–1379.
[52] C.-Y. Poon, H.-M. Chan, H.-W. Li, Direct detection of prostate specific antigen by darkfield microscopy using single immunotargeting silver nanoparticle, Sensors Actuat. B Chem. 190 (2014) 737–744.
[53] H.K. Choi, J.H. Lee, Role of magnetic Fe3O4 graphene oxide in chemiluminescent aptasensors capable of sensing tumor markers in human serum, Anal. Methods 5 (2013) 6964–6968.
[54] C. Kokkinos, A. Economou, P.S. Petrou, S.E. Kakabakos, Microfabricated tin-film electrodes for protein and DNA sensing based on stripping voltammetric detection of Cd (II) released from quantum dots labels, Anal. Chem. 85 (2013) 10686–10691.
[55] M.S. Chiriaco, E. Primiceri, A. Montanaro, F. de Feo, R. Rinaldi, G. Maruccio, On-chip screening for prostate cancer: an EIS microfluidic platform for contemporary detection of free and total PSA, Analyst 138 (2013) 5404–5410.
[56] N. Liu, W. Liang, X. Ma, X. Li, B. Ning, C. Cheng, G. Ou, B. Wang, J. Zhang, Z. Gao, Simultaneous and combined detection of multiple tumor biomarkers for prostate cancer in human serum by suspension array technology, Biosens. Bioelectron. 47 (2013) 92–98.
[57] L. Ding, J. You, R. Kong, F. Qu, Signal amplification strategy for sensitive immunoassay of prostate specific antigen (PSA) based on ferrocene incorporated polystyrene spheres, Anal. Chim. Acta 793 (2013) 19–25.
[58] S. Ge, J. Yu, X. Jiao, D. Chen, Ultrasensitive electrochemiluminescence immunoassay for protein specific detection based on dendrimer-encapsulated gold nanoparticles labels, J. Inorg. Organomet. Polym. 23 (2013) 1113–1121.
[59] C. Fernandez-Sanchez, C.J. McNeil, K. Rawson, O. Nilsson, Disposable noncompetitive immunosensor for free and total prostate-specific antigen based on capacitance measurement, Anal. Chem. 76 (2004) 5649–5656.
[60] X. Pei, Z. Xu, J. Zhang, Z. Liu, J. Tian, Redox-active and catalytic-efficient PAMAM dendrimer nanostructures for sensing low-abundance protein with signal amplification, Chem. Lett. 42 (2013) 841–842.
[61] D.-J. Kim, I.Y. Sohn, J.-H. Jung, O.J. Yoon, N.E. Lee, J.-S. Park, Reduced graphene oxide field-effect transistor for label-free femtomolar protein detection, Biosens. Bioelectron. 41 (2013) 621–626.
[62] G. Ertürk, D. Berillo, M. Hedström, B. Mattiasson, Microcontact-BSA imprinted capacitive biosensor for real-time, sensitive and selective detection of BSA, Biotechnol. Rep. 3 (2014) 65–72.

Please cite this article in press as: G. Ertürk, et al., Real-time prostate-specific antigen detection with prostate-specific antigen imprinted capacitive biosensors, Analytica Chimica Acta (2015), http://dx.doi.org/10.1016/j.aca.2015.07.055